

## Supporting Information

### **Pt-ligand Single-atom Catalysts: Tuning Activity by Oxide Support**

#### **Defect Density**

*Xuemei Zhou,<sup>[a]</sup> Linxiao Chen,<sup>[a]</sup> † George E. Sterbinsky,<sup>[b]</sup> Debangshu Mukherjee,<sup>[c]</sup>*

*Raymond R. Unocic,<sup>[c]</sup> Steven L. Tait<sup>[a]</sup>\**

<sup>[a]</sup> Dr. X. Zhou, Dr. L. Chen, Prof. S. L. Tait, Department of Chemistry, Indiana University, 800 E. Kirkwood Ave., Bloomington, Indiana 47405 (U. S. A.), E-mail: tait@indiana.edu;

<sup>[b]</sup> Dr. G. E. Sterbinsky, Advanced Photon Source, Argonne National Laboratory, 9700 S. Cass Ave., Lemont, Illinois 60439 (U. S. A.);

<sup>[c]</sup> Dr. D. Mukherjee, Dr. R. R. Unocic, Center for Nanophase Materials Sciences, Oak Ridge National Laboratory, 1 Bethel Valley Rd, Oak Ridge, TN 37830 (U.S.A.).

† Present address: Institute for Integrated Catalysis, Pacific Northwest National Laboratory, Richland, Washington 99352, USA

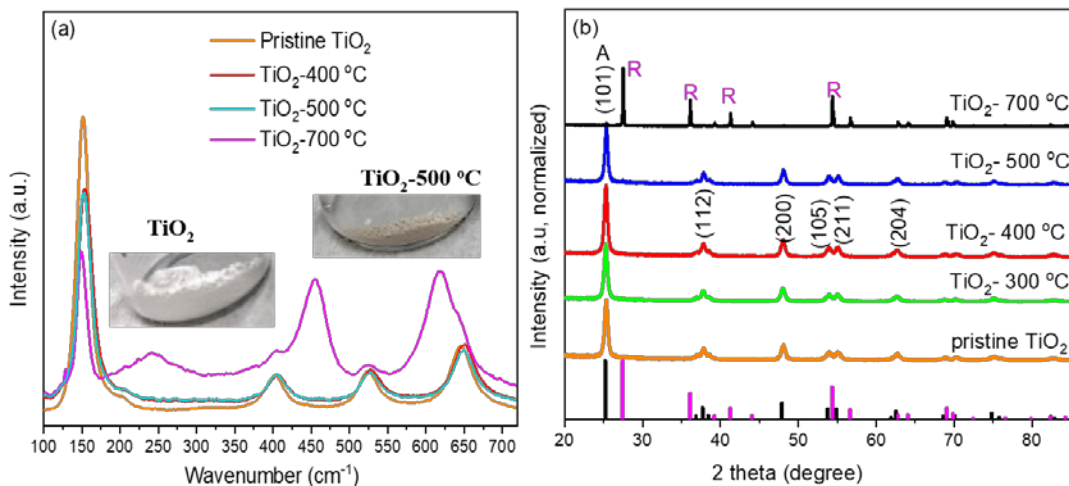


**Figure S1.** (a) Raman spectra under 514 nm laser irradiation at 298 K for pristine TiO<sub>2</sub> and TiO<sub>2</sub> annealed at 400 °C, 500 °C and 700 °C for 1h. Inset: Optical images of pristine TiO<sub>2</sub> and defective TiO<sub>2</sub> annealed at 500 °C for 1h. (b) Powder XRD patterns for TiO<sub>2</sub> nanoparticles and defective TiO<sub>2</sub> nanoparticles annealed at from 300°C to 700 °C for 1h in forming gas H<sub>2</sub>/N<sub>2</sub>, respectively. All the spectra are normalized to 25.27° for anatase (101) peak, except for sample annealed at 700 °C, which is normalized to 27.51° for rutile (110) peak. “A” refers to anatase phase and “R” refers to rutile phase.

**Table S1.** Particle size calculation based on Scherrer Equation from XRD results in **Figure S1b**.

Sample	Anatase (101)	Rutile (110)
Pristine TiO <sub>2</sub>	17.1 nm	-
TiO <sub>2</sub> -300 °C	17.0 nm	-
TiO <sub>2</sub> -400 °C	16.9 nm	-
TiO <sub>2</sub> -500 °C	16.9 nm	-
TiO <sub>2</sub> -700 °C	44.8 nm	156.4 nm

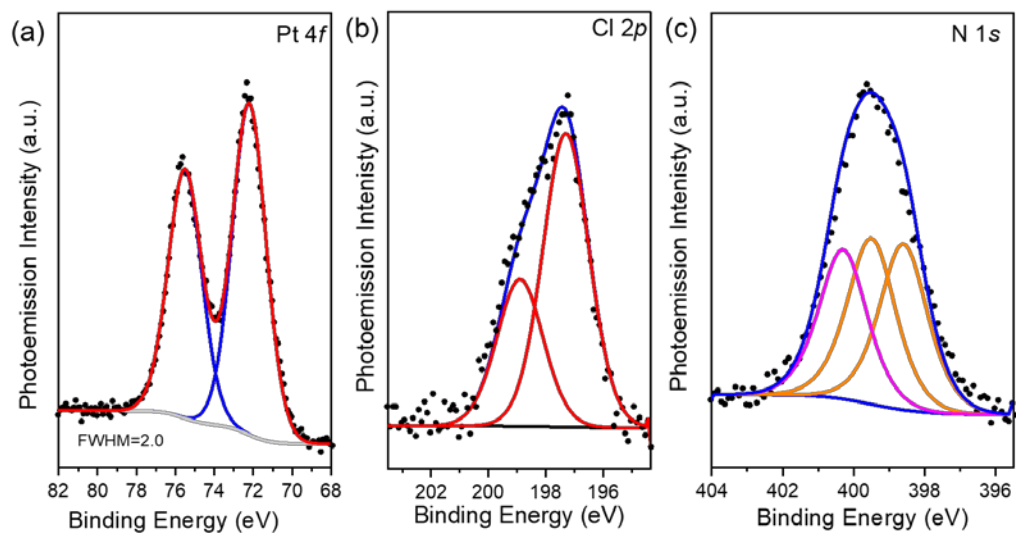


**Figure S2.** (a) Pt 4*f*, (b) Cl 2*p*, and (c) N 1*s* XP spectra with peak fitting for Pt SACs with DPTZ decorated on defective TiO<sub>2</sub> annealed at 700 °C.

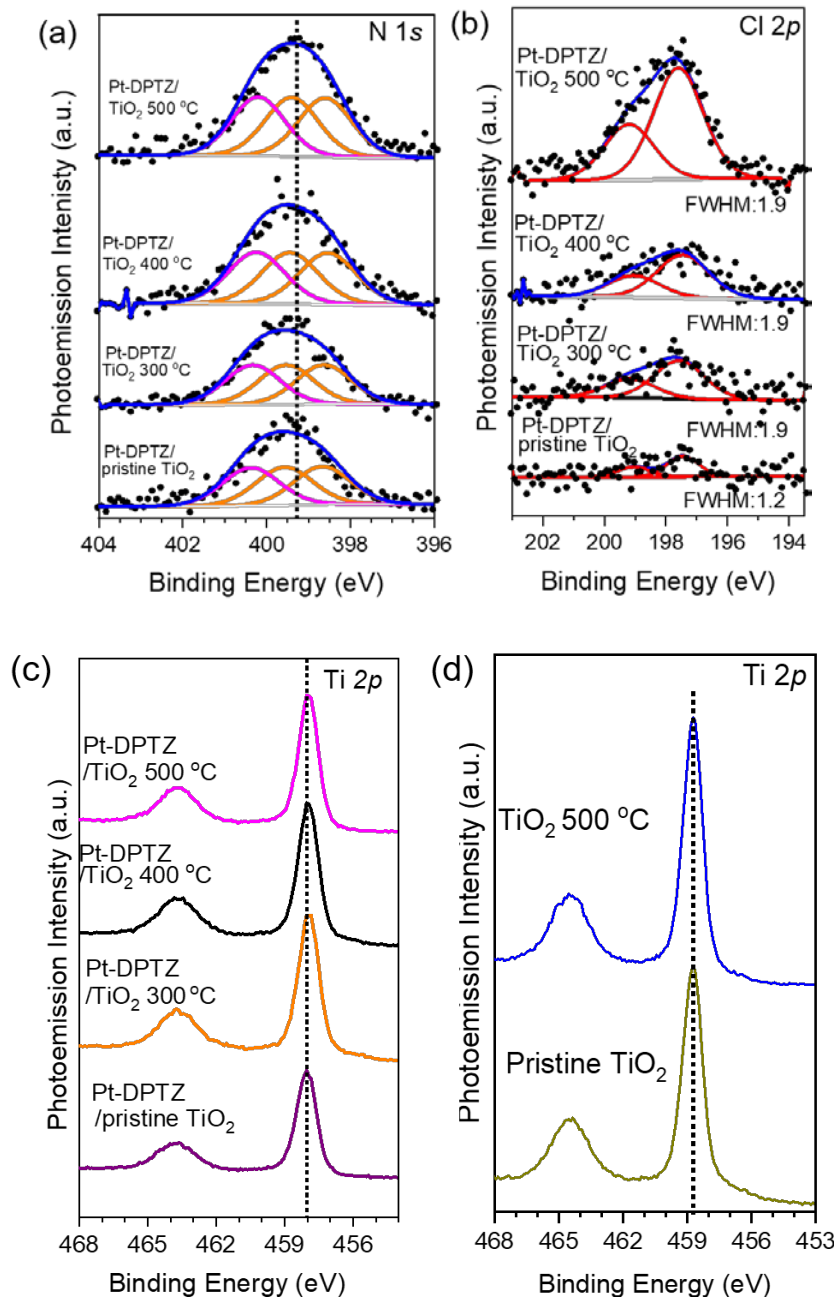


**Figure S3.** (a) N 1s, (b) Cl 2p, and (c) Ti 2p XPS spectra with peak fitting for Pt SACs with DPTZ decorated on pristine TiO<sub>2</sub>, on defective TiO<sub>2</sub> annealed at 300 °C, 400 °C and 500 °C. N 1s for pure DPTZ is also included as a reference. (d) Ti 2p spectra of pristine TiO<sub>2</sub>, and TiO<sub>2</sub> 500 °C (BE correction made by alignment to C 1s at 284.8 eV to resolve change in Ti 2p peaks). For all the Ti 2p peak, the Ti 2p<sub>1/2</sub> is located at the binding energy of 458.7, and Ti 2p<sub>3/2</sub> is located at 464.5 eV, which suggests these Ti is Ti<sup>4+</sup>. No clear Ti<sup>3+</sup> states are observed by XPS, which is located at 456.9 eV for Ti 2p<sub>1/2</sub> and 462.7 eV for Ti 2p<sub>3/2</sub>.<sup>1-2</sup>

**Table S2.** A summary of yield of product and turnover number for Pt-DPTZ on different TiO<sub>2</sub> support after reaction at 70 °C for 10 min.

	Pt ratio (% , ICP-MS)	Yield of product	TON
Pt-DPTZ/Pristine TiO <sub>2</sub> 1 <sup>st</sup> cycle	0.24	2.5	830
Pt-DPTZ/TiO <sub>2</sub> 300 °C 1 <sup>st</sup> cycle	0.54	1.1	220
Pt-DPTZ/TiO <sub>2</sub> 400 °C 1 <sup>st</sup> cycle	0.54	50.3	8470
Pt-DPTZ/TiO <sub>2</sub> 500 °C 1 <sup>st</sup> cycle	0.63	99.2	12530
Pt-DPTZ/TiO <sub>2</sub> 700 °C 1 <sup>st</sup> cycle	0.51	2.8	450

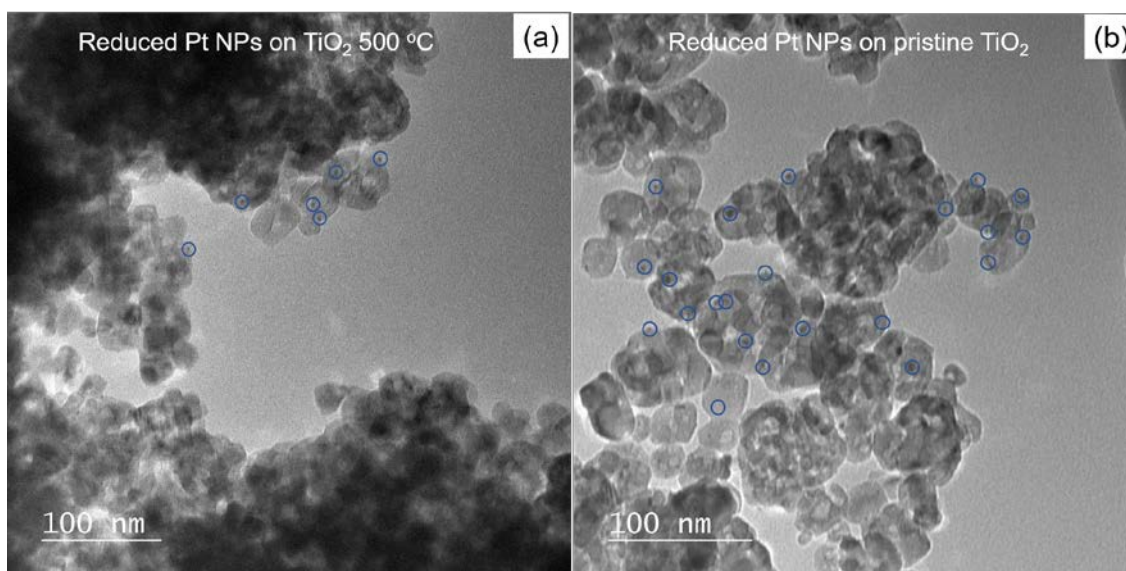


**Figure S4.** TEM images of reduced Pt nanoparticles on (a) TiO<sub>2</sub> 500 °C and on (b) pristine TiO<sub>2</sub>. After reduction at 400 °C for 1 h in H<sub>2</sub>/Ar, the Pt forms nanoparticles on the TiO<sub>2</sub> surfaces, which are approximately 3-4 nm in diameter.

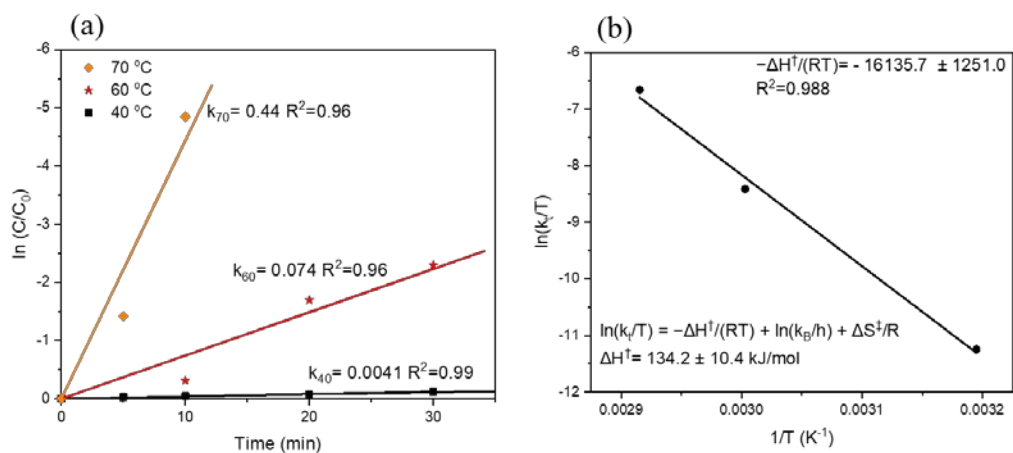


**Figure S5.** (a) Calculation and comparison of the apparent reaction rate constant ( $k$ ) at different temperatures from concentration time profile data (for data below full conversion). (b) Calculation of reaction activation energy based on first order reaction rate constant from (a) for Pt-DPTZ SACs on  $\text{TiO}_2$  annealed at 500 °C. The calculation is based on the Eyring Equation, displayed in (b).

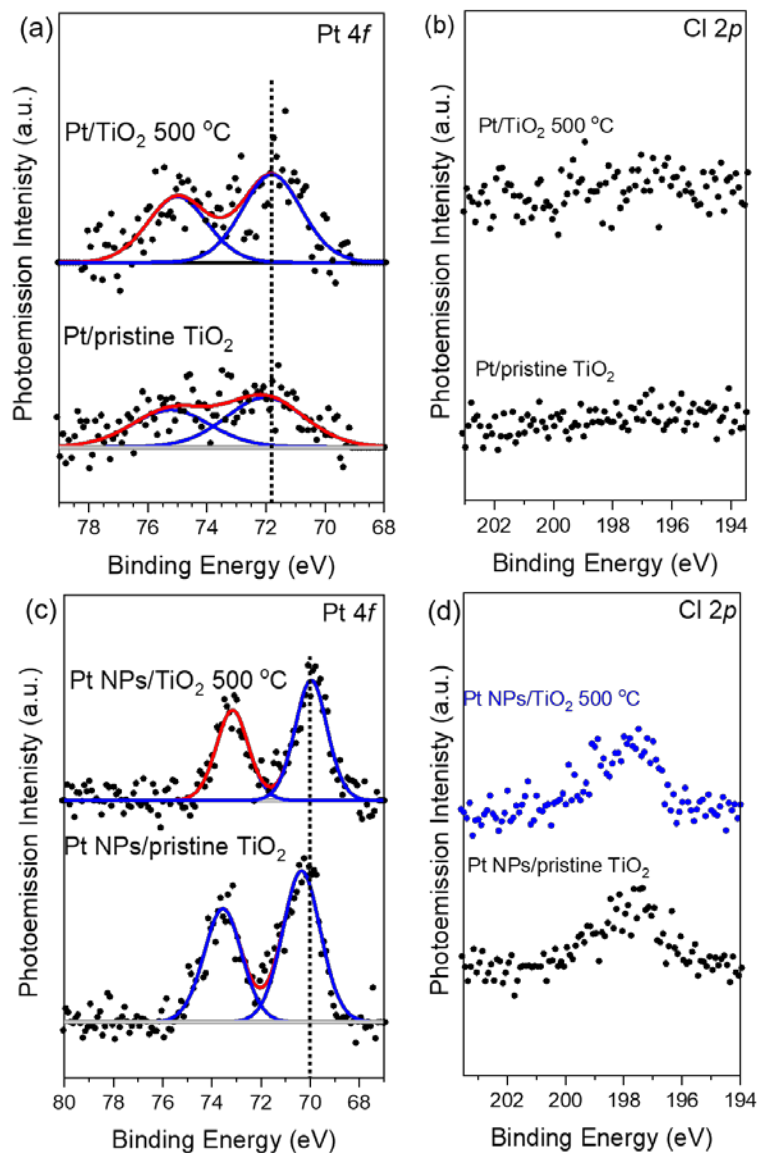


**Figure S6.** (a) Pt 4*f* with peak fitting and (b) Cl 2*p* XP spectra for bare Pt on pristine TiO<sub>2</sub> (bottom) and on defective TiO<sub>2</sub> (500 °C anneal), showing the Pt has wide distribution on pristine surface (FWHM=3.1) than on defective TiO<sub>2</sub> (500 °C anneal) surface (FWHM=2.4). (c) Pt 4*f* with peak fitting and (d) Cl 2*p* XP spectra for reduced Pt NPs on pristine TiO<sub>2</sub> (bottom) and on defective TiO<sub>2</sub> (500 °C anneal). The reduced Pt has a binding energy of 70.0 eV for Pt 4*f*<sub>7/2</sub> for Pt NPs on TiO<sub>2</sub> (500 °C), and a binding energy of 70.4 eV for Pt NPs on pristine TiO<sub>2</sub>. The 0.4 eV lower binding energy of Pt on defective TiO<sub>2</sub> support is ascribed to the strong metal support interaction, than on pristine surface.<sup>3-4</sup>

**Table S3.** EXAFS fitting parameters for Pt-DPTZ on pristine TiO<sub>2</sub>, Pt-DPTZ on TiO<sub>2</sub> annealed at 500 °C, and Pt-DPTZ on pristine TiO<sub>2</sub> after hydrosilylation reaction, as shown in **Figures 4a, 4b, and 4c**, respectively. Two sets of fitting parameters are compared here: the top table shows fitting using Pt-Cl and Pt-N paths and the bottom table shows fitting using Pt-Cl and Pt-O paths. The former set of fitting is slightly better in fit quality and was used in **Figure 4**. One standard deviation is given in parentheses. The *k* ranges for Fourier transformation are selected to be 3 to 11.3 Å<sup>-1</sup> for Pt-DPTZ/pristine TiO<sub>2</sub>, 3 to 12 Å<sup>-1</sup> for Pt-DPTZ/TiO<sub>2</sub> 500 °C and 3 to 8.2 Å<sup>-1</sup> for Pt-DPTZ/pristine TiO<sub>2</sub> post reaction sample based on the signal to noise at high *k*. The *N* (Pt-Cl) value, when set as a free fitting parameter, is close to the measured Cl/Pt ratio in XPS. It was fixed at that value in the final fitting to reduce the number of free parameters. Pt-DPTZ/TiO<sub>2</sub> 500 °C was not measured after hydrosilylation reaction.

Fitting parameter/Catalysts	Pt-Cl			Pt-N			Reduced $\chi^2$	R-factor
	<i>N</i>	<i>R</i> (Å)	$\sigma^2$ (10 <sup>-3</sup> )	<i>N</i>	<i>R</i> (Å)	$\sigma^2$ (10 <sup>-3</sup> )		
Pt-DPTZ/pristine TiO <sub>2</sub>	0.6	2.30 (± 0.03)	1 (± 0.4)	4.7 (± 0.9)	2.03 (± 0.01)	8 (±3)	48	0.052
Pt-DPTZ/TiO <sub>2</sub> 500 °C	1.4	2.30 (± 0.01)	1 (± 1)	3.2 (± 0.4)	2.03 (± 0.01)	5 (± 2)	46	0.011
Pt-DPTZ/pristine TiO <sub>2</sub> (post reaction)	–*	–	–	5.2 (± 0.9)	2.05 (± 0.01)	9 (± 3)	28	0.022
	Pt-Cl			Pt-O				
	<i>N</i>	<i>R</i> (Å)	$\sigma^2$ (10 <sup>-3</sup> )	<i>N</i>	<i>R</i> (Å)	$\sigma^2$ (10 <sup>-3</sup> )	59	0.061
Pt-DPTZ/pristine TiO <sub>2</sub>	0.6	2.30 (± 0.04)	1 (± 4)	5.0 (± 1.4)	2.01 (± 0.01)	9 (±5)	67	0.017
Pt-DPTZ/TiO <sub>2</sub> 500 °C	1.4	2.30 (± 0.01)	1 (± 1)	3.5 (± 0.6)	2.01 (± 0.01)	6 (± 3)	58	0.044
Pt-DPTZ/pristine TiO <sub>2</sub> (post reaction)	–*	–	–	5.7 (± 1.6)	2.02 (± 0.01)	11 (± 5)	58	0.044

\* Pt-DPTZ/pristine TiO<sub>2</sub> post-reaction shows a significant decrease in XPS Cl signal. If the XPS Cl/Pt ratio (0.3) is used as the *N* (Pt-Cl) fitting parameter, the EXAFS peak fit is relatively poor (high reduced chi-square value and R-factor) compared to omitting the Pt-Cl path, which is what was done in the final fitting. This indicates that the residual Cl detected in XPS seems, according to EXAFS, to not be coordinated directly to Pt. In the two pre-reaction cases in the table, the XPS Cl/Pt ratio matches closely with the *N* (Pt-Cl) fitting result.

**Table S4.** Alternate EXAFS fitting for Pt-DPTZ on pristine TiO<sub>2</sub>, Pt-DPTZ on TiO<sub>2</sub> annealed at 500 °C, and Pt-DPTZ on pristine TiO<sub>2</sub> after hydrosilylation reaction (data plotted in **Figures 4a, 4b, and 4c**). This fitting model differs from those in **Table S3** because of the inclusion of the Pt-Pt path. As shown in the table, the fit quality of this model is poor and the coordination number for Pt-Pt is very small.

Fitting parameter/ Catalysts	Pt-Cl			Pt-N			Pt-Pt			Reduced $\chi^2$	R-factor
	<i>N</i>	<i>R</i> (Å)	$\sigma^2$ (10 <sup>-3</sup> )	<i>N</i>	<i>R</i> (Å)	$\sigma^2$ (10 <sup>-3</sup> )	<i>N</i>	<i>R</i> (Å)	$\sigma^2$ (10 <sup>-3</sup> )		
Pt-DPTZ/ pristine TiO <sub>2</sub>	0.6	2.29 (± 0.05)	1 (± 6)	7.3 (± 2.1)	2.03 (± 0.03)	9 (± 5)	<b>0.1</b> (± <b>0.5</b> )	2.82 (± 0.04)	<b>-11</b> (± <b>20</b> )	60	0.009
Pt-DPTZ/TiO <sub>2</sub> 500 °C	1.4	2.31 (± 0.02)	1 (± 2)	5.5 (± 1.7)	2.04 (± 0.03)	6 (± 5)	<b>-4.2</b> (± <b>19.5</b> )	2.93 (± 0.2)	<b>29</b> (± <b>92</b> )	206	0.009
Pt-DPTZ/ pristine TiO <sub>2</sub> (post reaction)	-	-	-	9.4 (± 4.4)	2.05 (± 0.02)	14 (± 9)	<b>0.1</b> (± <b>1.2</b> )	2.59 (± 0.1)	<b>-20</b> (± <b>79</b> )	91	0.006

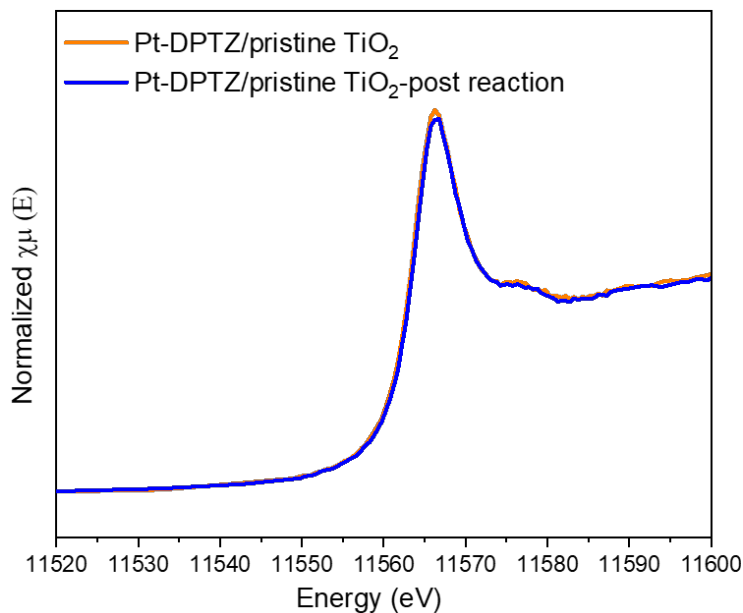


**Figure S7.** Pt *L*<sub>3</sub> edge XANES for Pt-DPTZ SACs on pristine TiO<sub>2</sub> before and after hydrosilylation reaction for one cycle.

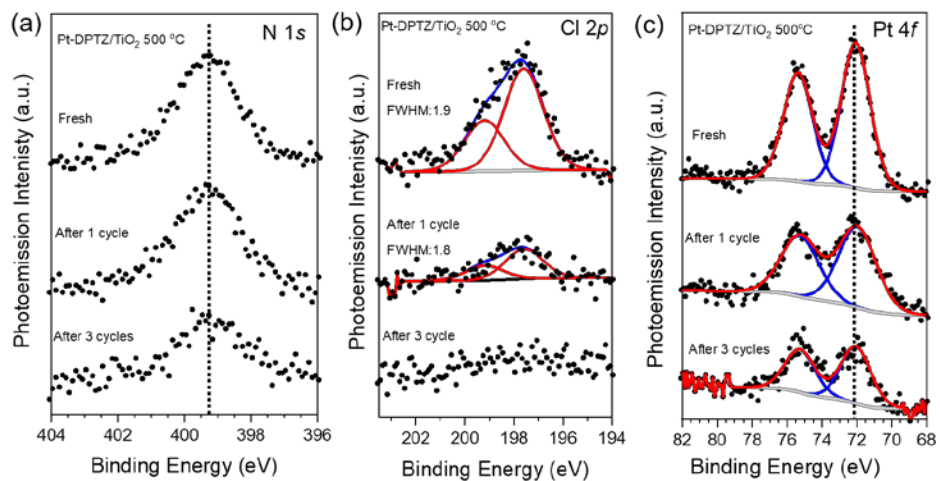


**Figure S8.** (a) N 1s, (b) Cl 2p, and (c) Pt 4f XPS spectra with peak fitting for Pt-DPTZ SACs on defective TiO<sub>2</sub> (annealed at 500 °C) after hydrosilylation reaction for one cycle, and 3 cycles.

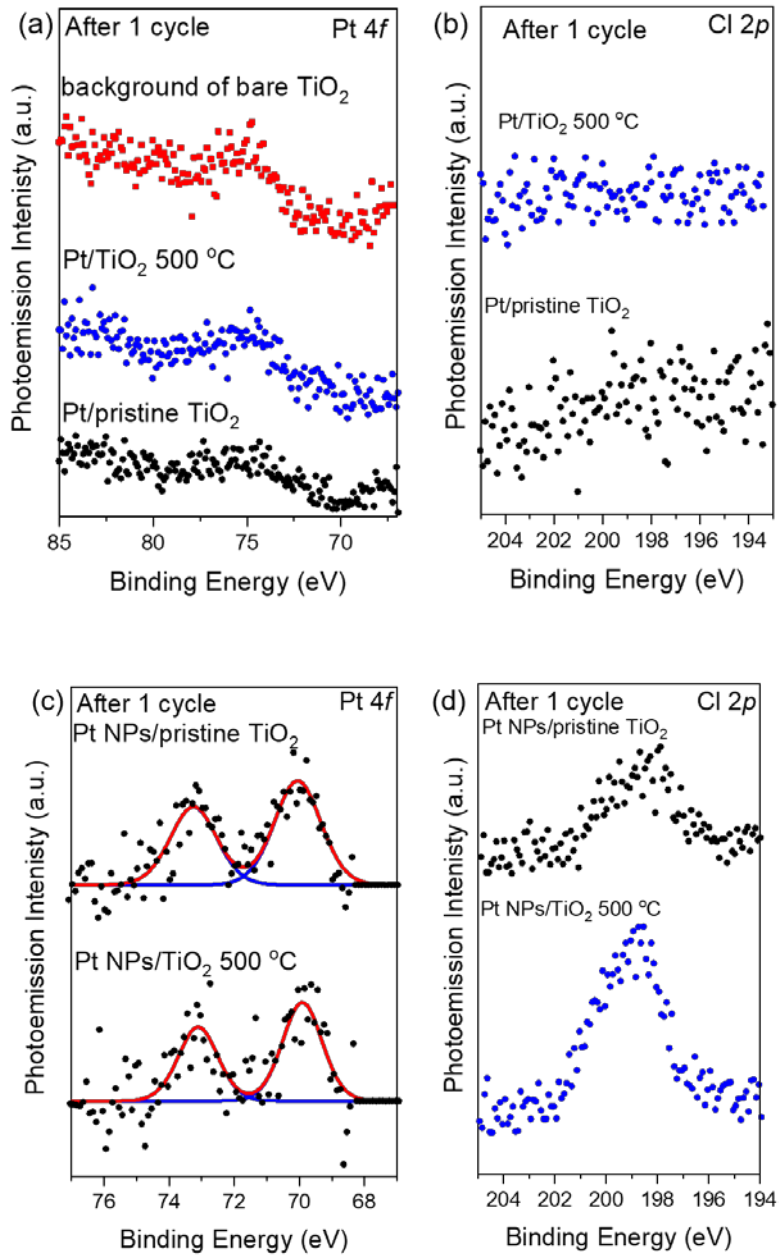


**Figure S9.** (a) Pt 4*f* XPS spectra and (b) Cl 2*p* for bare Pt after hydro-silylation reaction at 70 °C for 30 min for one cycle. Red curve in **Figure S9a** is the background of bare TiO<sub>2</sub> at this region. After 1 cycle of reaction, hardly Pt is detected from XPS of these two samples. (c) Pt 4*f* XPS spectra and (d) Cl 2*p* for supported Pt NPs after hydro-silylation reaction at 70 °C for 30 min for one cycle.

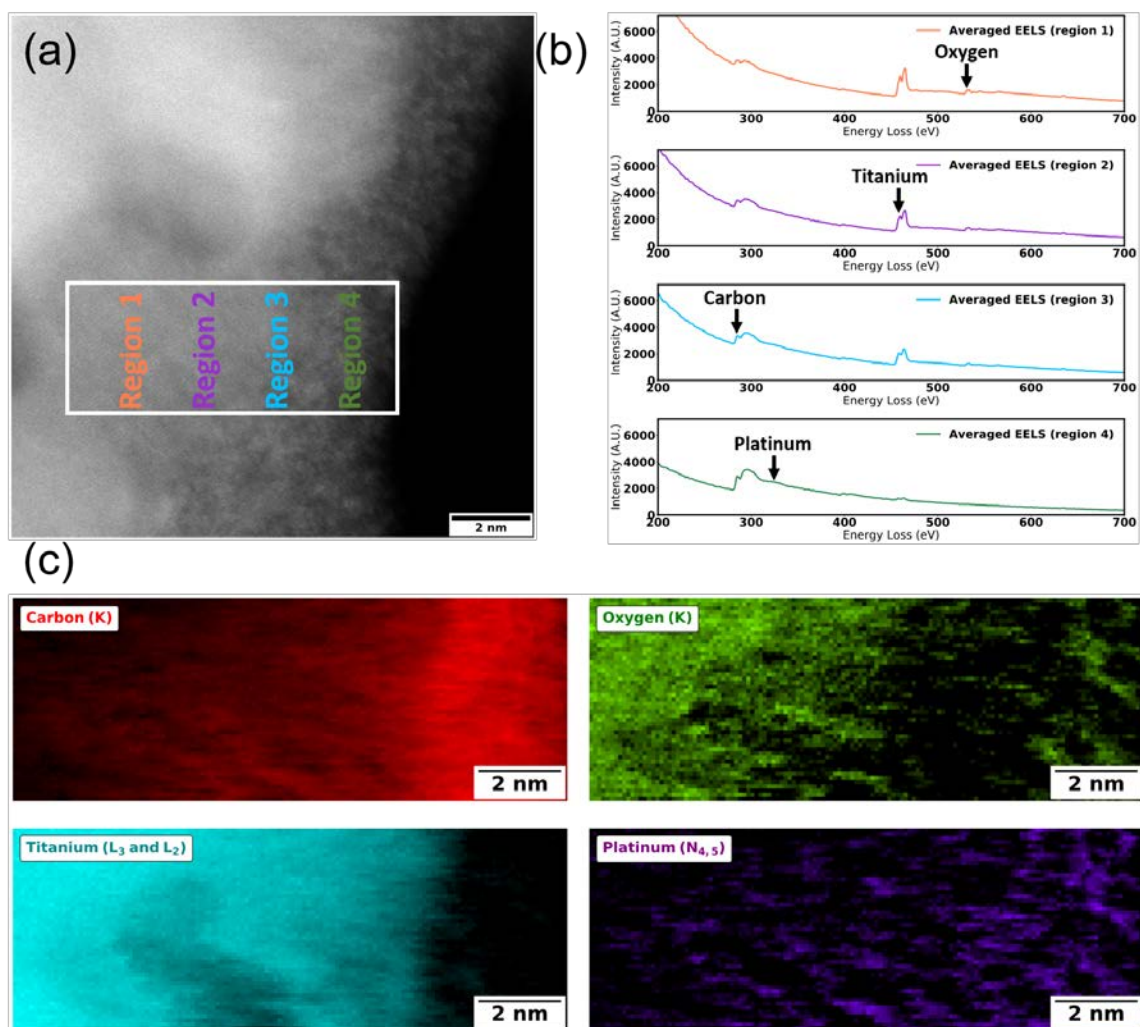


**Figure S10.** (a) HAADF-STEM Image for Pt-DPTZ/TiO<sub>2</sub> 500 °C for EELS analysis, with the white box showing the EELS elemental analysis area, which is divided into four regions. Note that in Regions 1 and 2, the STEM image shows rows of the crystalline TiO<sub>2</sub>, but that the ordering is less prominent in Regions 3 and 4. (b) EELS spectra from the regions marked in (a), showing the presence of carbon, titanium, oxygen and platinum (N<sub>4,5</sub> peak). (c) Elemental maps for carbon (red), oxygen (green), titanium (blue), and platinum (purple) from the region marked by the white box in (a). Carbon and platinum are observed in the less-ordered region 4 at a significantly higher concentration than in the ordered TiO<sub>2</sub> regions 1 and 2, consistent with Figure 8. Note that the Pt signal is quite weak due to low Pt concentration, but does not indicate any significant Pt clustering, consistent with the EXAFS results.

## References

1. Zhou, X.; Liu, N.; Schmuki, P., Ar<sup>+</sup>-ion bombardment of TiO<sub>2</sub> nanotubes creates co-catalytic effect for photocatalytic open circuit hydrogen evolution. *Electrochem. Commun.* **2014**, *49*, 60-64.
2. Jackman, M. J.; Thomas, A. G.; Muryn, C., Photoelectron Spectroscopy Study of Stoichiometric and Reduced Anatase TiO<sub>2</sub>(101) Surfaces: The Effect of Subsurface Defects on Water Adsorption at Near-Ambient Pressures. *J. Phys. Chem. C* **2015**, *119*, 13682-13690.
3. A Dauscher, L. H., F. Le Normand, W. Müller, G. Maire and A. Vasq wz, Characterization by XPS and XAS of Supported Pt/TiO<sub>2</sub>-CeO<sub>2</sub> Catalysts. *Surface and Interface Analysis.* **1990**, *16*, 34-346.
4. Tauster, S. J.; Fung, S. C.; Garten, R. L., Strong Metal-Support Interactions. Group 8 Noble Metals Supported on TiO<sub>2</sub>. *J. Am. Chem. Soc.* **1978**, *100*, 170-175.